RAPID COMMUNICATION

Direct observation of the carrier transport process in InGaN quantum wells with a pn-junction*

Haiyan Wu(吴海燕)†, Ziguang Ma(马紫光)†, Yang Jiang(江洋), Lu Wang(王禄), Haojun Yang(杨浩军), Yangfeng Li(李阳锋), Peng Zuo(左朋), Haiqiang Jia(贾海强), Wenxin Wang(王文新), Junming Zhou(周钧铭), Wuming Liu(刘伍明), and Hong Chen(陈弘)‡

Key Laboratory for Renewable Energy, Beijing Key Laboratory for New Energy Materials and Devices, Beijing National Laboratory for Condensed Matter Physics, Institute of Physics, Chinese Academy of Sciences, Beijing 100190, *China*

(Received 16 August 2016; published online 28 September 2016)

A new mechanism of light-to-electricity conversion that uses InGaN/GaN QWs with a p–n junction is reported. According to the well established light-to-electricity conversion theory, quantum wells (QWs) cannot be used in solar cells and photodetectors because the photogenerated carriers in QWs usually relax to ground energy levels, owing to quantum confinement, and cannot form a photocurrent. We observe directly that more than 95% of the photoexcited carriers escape from InGaN/GaN QWs to generate a photocurrent, indicating that the thermionic emission and tunneling processes proposed previously cannot explain carriers escaping from QWs. We show that photoexcited carriers can escape directly from the QWs when the device is under working conditions. Our finding challenges the current theory and demonstrates a new prospect for developing highly efficient solar cells and photodetectors.

Keywords: p–n junction, carrier transportation, quantum wells, light-to-electricity conversion

PACS: 78.67.Lt, 73.40.–c, 72.20.–I **DOI:** 10.1088/1674-1056/25/11/117803

1. Introduction

The p–n junction is an essential component of most light-to-electricity conversion devices, such as solar cells and photodetectors. Among these devices are silicon solar cells,[1] GaAs-based concentrator photovoltaic systems,[2] CdTe and CuInGaSe film solar cells,[3,4] InAsSb, HgCdTe, and InAs/GaSb superlattice-based infrared detectors,[5,6] and AlGaN, SiC, and ZnO based ultraviolet detectors,[7–9] all of which have found extensive applications in information technology. On the other hand, quantum wells (QWs) with the one-dimensional (1D) quantum confinement effect have been applied extensively in electricity-to-light devices such as light-emitting diodes and lasers. However, they cannot be used in devices that convert light to electricity by means of interband transition. This is because, according to the well established theory,[10,11] the photo-generating carriers are restricted to the ground energy level and cannot escape from QWs to an external circuit to form photocurrent. Recently, the insertion of multiple QWs (MQWs) into the depletion region of a p–n junction was reported to extend the range of spectral response and increase the photocurrent of solar cells.[12] This photoexcited carrier escape phenomenon was explained by thermionic emission and tunneling processes.[13–15] However, whether the theory works has not been meticulously tested by experiment. One of the main reasons is that the carrier transport process in a device is difficult to access and investigate experimentally.

In this paper, we report solving this problem and clarifying the photoexcited carrier escape phenomena in QWs by conducting simultaneous measurements of resonant excitation photoluminescence, photocurrent, and photovoltage under both open- and short-circuit conditions for InGaN/GaN QWs with a p–n junction. It is found that more than 95% of the photo-excited carriers escape from the QWs and form photocurrent by interband transition. Our discovery not only challenges the theory, but also demonstrates a new mechanism that might well enable applying QWs in solar cells and photodetectors.

2. Experiment

Two different MQW structures, shown in Fig. 1, are used to investigate PL spectra and light-to-electricity conversion. The first device (Fig. 1(a)) consists of InGaN/GaN MQWs in a p–n junction, and the second (Fig. 1(b)) has a similar structure except that the p–n junction is replaced by an n-n junction; they are referred to hereafter as device A and device B, respectively. After epitaxial growth, chips with a size of 1 mm×1 mm were fabricated for electrical measurements. A 405-nm laser beam was used as the excitation source. The photon energy 3.06 eV of the laser lies between the bandgap (2.7 eV) of the InGaN QW and that (3.4 eV) of the GaN bar-

*Project supported by the National Natural Science Foundation of China (Grant Nos. 11574362, 61210014, and 11374340) and the Innovative Clean-energy Research and Application Program of Beijing Municipal Science and Technology Commission, China (Grant No. Z151100003515001).

†These authors contributed equally to this work.

‡Corresponding author. E-mail: hchen@iphy.ac.cn

© 2016 Chinese Physical Society and IOP Publishing Ltd

rier. The situation is known as the resonant excitation.[16] The photoexcited carriers are only generated in the InGaN QWs and should be restricted by the GaN barrier.

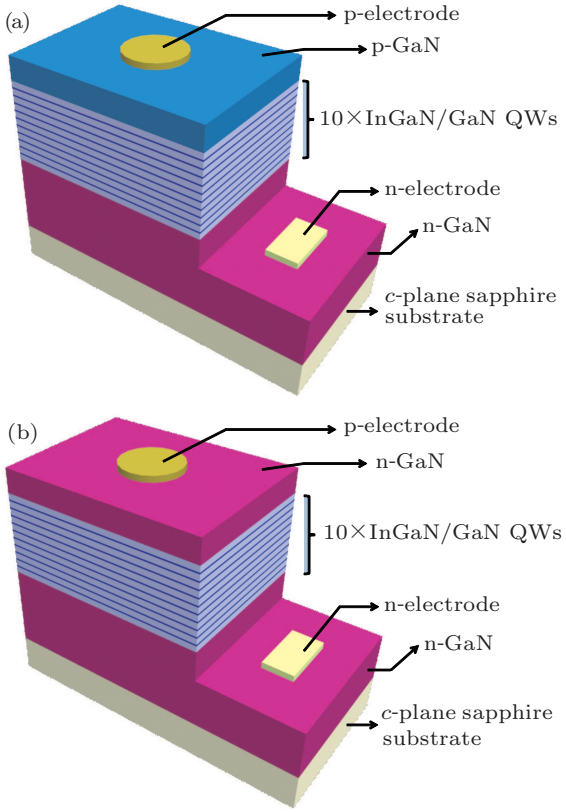


Fig. 1. (color online) (a) Schematic of device A. The InGaN/GaN MQWs are the active region and are sandwiched between p-type and n-type GaN; each MQW consists of a 2.5 nm InGaN well and a 12 nm GaN barrier layer. (b) Schematic of device B, which is deposited similarly, except that the p-GaN is replaced by an equal thickness of n-GaN.

3. Results and discussion

Under an excitation power of 27 mW, the measured open-circuit photovoltage of device A is 2.452 V and the PL spectrum centers at 456.5 nm under open-circuit conditions. For the same excitation power, the short-circuit photocurrent is 3.38 mA and the peak wavelength exhibits a blue shift by 3.7 nm to 452.8 nm under short-circuit conditions. Surprisingly, as shown in Fig. 2(a), the integrated PL intensity (blue curve) under short-circuit conditions is significantly reduced more than twentyfold to 4.85% of the intensity under open-circuit conditions.

To investigate the difference between the two conditions, we measured the excitation-power-dependence of the integrated PL intensity and peak wavelength parameters up to a maximum excitation power of 27 mW. As the excitation power increases, several features are observed under open-circuit conditions: a nearly linear increase in the integrated PL intensity (empty triangles, Fig. 2(b)), a blue shift of the PL peak wavelength from 458.2 nm to 456.5 nm (open balls, Fig. 2(b)), as well as an exponentially increasing photovoltage from 2.366 V to 2.452 V (upper panel, Fig. 2(c)). Different behaviors are observed under short-circuit conditions: a very weak parabolic increase in the integrated PL intensity (solid triangles, Fig. 2(b)) and a linear increase to 3.38 mA in the photocurrent. On the other hand, the PL peak wavelength (solid circles, Fig. 2(b)) shows a blue shift from 455.0 nm to 453.0 nm similar to that in the open-circuit case. The linear increase of the short-circuit photocurrent agrees with the law of light-to-electricity conversion.[17] The ratio of the

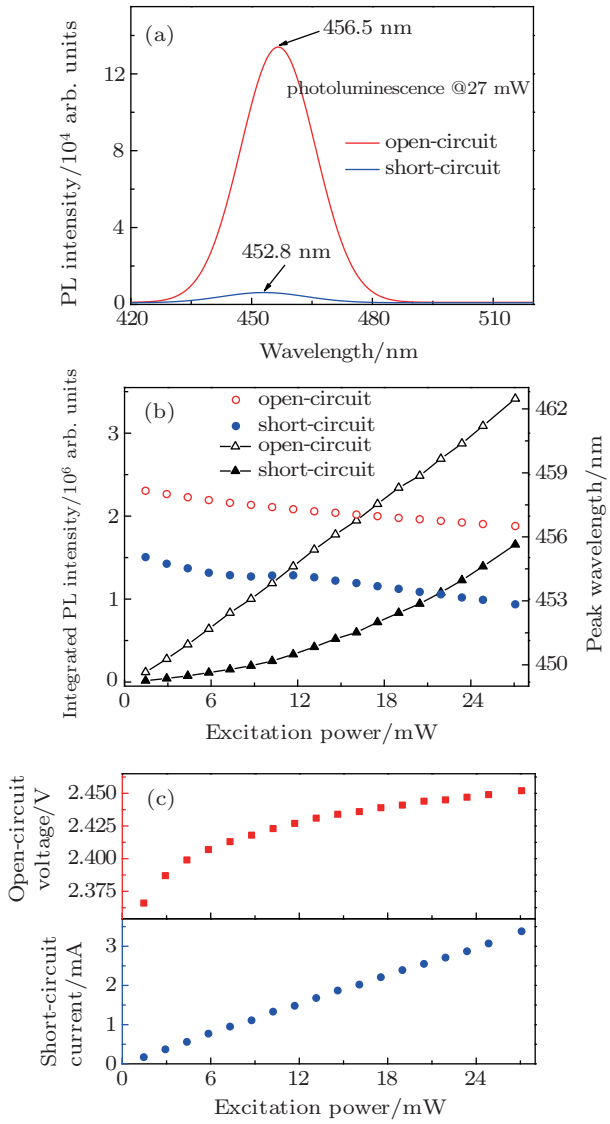


Fig. 2. (color online) PL spectra and light-to-electricity conversion results for device A under resonant excitation of 405 nm laser. (a) PL spectra under both short-circuit and open-circuit conditions with a 27 mW excitation power. Under open-circuit conditions, the measured open-circuit voltage is 2.452 V. Under short-circuit conditions, the peak wavelength of the PL spectrum shows a blue shift, and the measured short-circuit current is 3.38 mA. The device under short-circuit conditions exhibits much weaker emission, and the integrated PL intensity is reduced to 4.85% of that under open-circuit conditions. (b) The excitation-power-dependent integrated PL intensities and peak wavelength. The ratio of the integrated PL intensity under short-circuit conditions to that under open-circuit conditions shows a monotonic increase from 1.42% to 4.85%. (c) Plots showing the excitation-power-dependent open-circuit voltage and short-circuit current. The open-circuit voltage increases exponentially with increasing excitation power, whereas the short-circuit current increases linearly with increasing excitation power.

short-circuit PL intensity to the open-circuit one shows a monotonic increase from 1.42% to 4.85%; thus, more than 95% of the photoexcited carriers have escaped from the QWs to generate the photocurrent. This result reveals that QWs can be used in light-to-electricity conversion devices. For a 27 mW excitation power, the short-circuit current is 3.38 mA. The incident-photon-to-current conversion efficiency is therefore 38.3%.

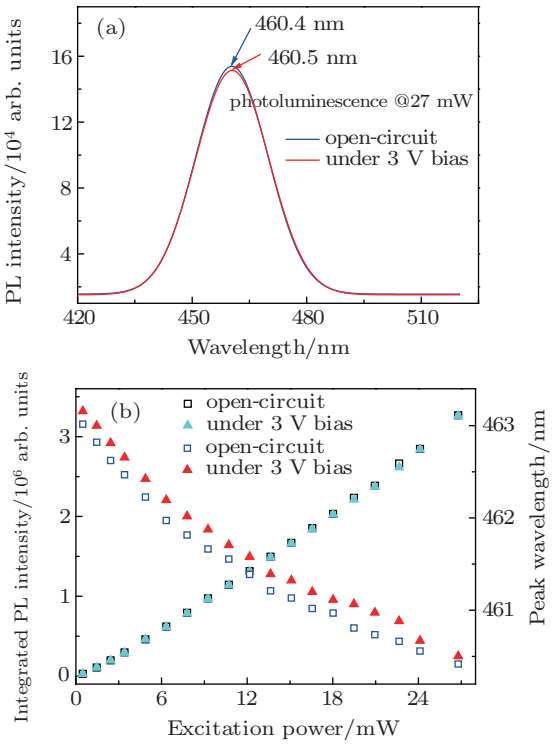


Fig. 3. (color online) PL spectra and light-to-electricity conversion results for device B under resonant excitation of 405 nm laser. (a) The PL spectra under open-circuit and 3 V bias conditions with a 27 mW excitation power. Compared with that under open-circuit conditions, the integrated PL intensity under 3 V bias is only 0.18% less. (b) The excitation-power-dependent integrated PL intensities and peak wavelengths under open-circuit and 3 V bias conditions. The integrated PL intensity under 3 V bias is only a few per millage less for the same excitation power.

Device B was further used to investigate the origin of the photocurrent generated in device A. Here an external 3 V bias on the chip was used to simulate the built-in field in device A. As shown in Fig. 3(a), for a 27 mW excitation power, the peak wavelength is 460.4 nm under open-circuit conditions. Applying 3 V bias leads to nearly no change: the peak position is at 460.5 nm. Likewise, there is only 0.18% change in the integrated PL intensity (solid triangles, Fig. 3(b)) compared with that (open squares, Fig. 3(b)) under open-circuit conditions in device B, which is significantly smaller than that in device A (Fig. 3(b)). We further studied the excitation-power-dependent PL, and the result is also shown in Fig. 3(b). With increasing excitation power, the integrated PL intensity exhibits a linear behavior under both conditions (open-squares and solid-triangles, Fig. 3(b)), and the difference between the two conditions is nearly invisible. The subtle decrease in the integrated PL intensity is due to energy-band inclination when the chip is under 3 V bias.[18] Additionally, the peak position shows a monotonic decrease from 463.0 nm to 460.4 nm under open-circuit conditions as well as from 463.2 nm to 460.5 nm under 3 V bias conditions. The above results support the hypothesis that the photoexcited carriers in device B fail to escape from the QWs, but instead recombine to emit light. This result is consistent with the theory that photoexcited carriers relax to the ground state of QWs.[10,11,19]

Comparing the results of the two devices, which possess the same barrier height and thickness, reveals that the photoexcited carriers' direct escape from the QWs to generate a photovoltaic effect is induced by the p–n junction. Meanwhile, the thermionic emission and tunneling processes cannot be used to explain the photoexcited carriers escaping from the QWs. The distinct behaviors in the carrier transport process in device A suggest that the photoexcited free carriers in a high excitation state must directly escape from the InGaN QWs in the p–n junction so as to generate the photovoltaic effect. If they relax to the ground state owing to the quantum confinement effect, the state cannot be changed by an electric field. Thus, we should not have observed the significant decrease in PL intensity shown in Fig. 2. We speculate that under open-circuit conditions, the free carriers in a high excitation state that are produced immediately after photon absorption in device A are not confined by the barriers but instead drift to the p-side or the n-side of the junction. This process leads to an increase in the potential of the p-type region and a decrease in the potential of the n-type region.[17] In this way, a photo-electromotive force is generated. Under open-circuit conditions, the photogenerated carriers, both e_1 and h_1 as shown in Fig. 4(a), are prevented from escaping from the QWs and relax to the ground states of the QW by phonon emission.[20,21] The carriers then recombine to emit photons with energy $h\nu_2$, which is smaller than the incident photon energy $h\nu_1$. Under closed-circuit conditions, the photogenerated electron pairs e and hole pairs h, shown in Fig. 4(b), directly escape from the QWs and generate a photocurrent in the circuit. Our mechanism for carriers escaping QWs is totally different from the mechanisms proposed before, such as thermionic emission and tunneling processes, which are based on the well-established light-to-electricity theory, i.e., the photoexcited carriers relax to the ground state of the QW first.

Considering GaN materials with an electron mobility of several hundred $cm^2 \cdot V^{-1} \cdot s^{-1}$,[22,23] a hole mobility of several $cm^2 \cdot V^{-1} \cdot s^{-1}$,[24,25] a quantum well width of 2.5 nm, and a built-in voltage greater than 2 V, the transit time of the photoexcited carriers over the quantum well in device A is on the order of femtoseconds.[26] In contrast, the relaxation time of the photoexcited carriers in InGaN quantum wells has been

reported to be approximately several picoseconds.[27] Given that the transit time is shorter than the relaxation time, the free carriers in a high excitation state directly escape from the quantum wells. Electron mobility is larger than hole mobility when a bias is applied in a QWs structure. Since the electric field distribution is nearly uniform in the undoped region, the drift velocity of electron is larger than that of hole. This phenomenon results in the escape of the photoexcited electrons from the QW region as well as the gathering of excess photoexcited holes in the QW region. This in turn prevents carriers from escaping. However, the distribution of electric field in p–n junctions can be adjusted by the doping concentration to maintain the same number of holes and electrons that flow out of the QW region, so as to assure the QWs region is electrically neutral. In this case, carriers easily escape from QWs.

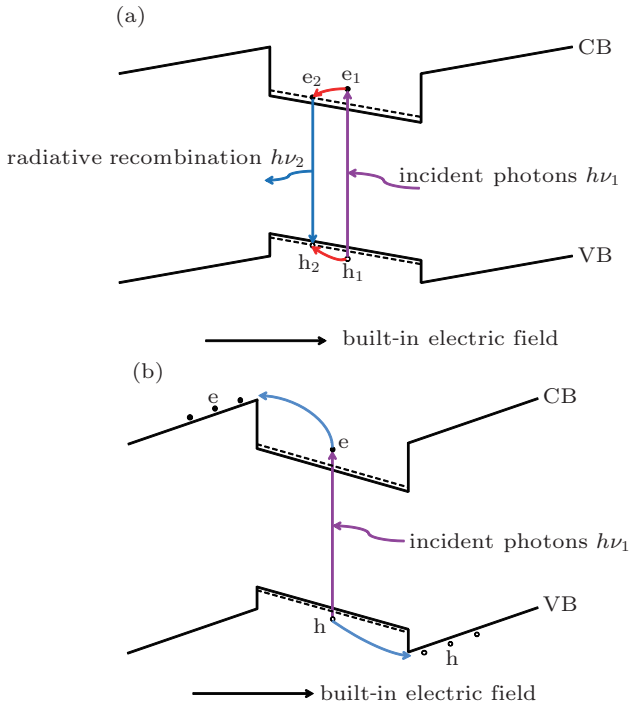


Fig. 4. (color online) Schematic of the light-to-electricity conversion process in device A. (a) Schematic diagram of energy band, absorption, and transport process of photo-generated carriers under open-circuit conditions. Under incident photon $h\nu_1$ interaction, a high-excitation state free electron–hole pair is generated, with the electron and hole separately escaping from the quantum well and generating a photovoltage. Under equilibrium conditions, most photoexcited free carriers such as e_1 and h_1 relax to ground state e_2 and h_2 to emit light. (b) Schematic diagram of energy band, absorption, and transport process of photo-generated carriers under short-circuit conditions. Under incident photon $h\nu_1$ interaction, high excitation state photo-excited free electron e and hole *h* directly escape from the QWs and generate a photocurrent.

4. Conclusion

We have demonstrated a new mechanism using InGaN QWs in a p–n junction potentially applicable in solar cells and photodetectors. It is found that the application of InGaN QWs would not only make the design of solar cells more flexible, but could also extend/select the spectral response range of photodetectors by using quantum confinement. It is envisioned that the mechanism can be extended to other quantum well structures since the fundamental band-alignment and light adsorption process are essentially the same.

Appendix A: Methods

Epitaxial growth Both structures were deposited on *c*-plane sapphire by metal–organic chemical vapor deposition (MOCVD). Trimethylgallium (TMGa), triethylgallium (TEGa), trimethylindium (TMIn), and ammonia (NH_3) were used as precursors, and silane (SiH_4) and dicyclopentadienyl magnesium (Cp_2Mg) were used as n-type and p-type dopants, respectively. After being annealed under an H_2 atmosphere at 1050 °C, a 25-nm-thick GaN nucleation layer was deposited onto the substrates at 530 °C and subsequently annealed at 1080 °C under an NH_3 atmosphere. The deposition of GaN was followed by the deposition of a 4 μm Si-doped GaN layer (electron concentration $= 2 \times 10^{18}$ cm^{-3}) at 1130 °C. Then, 10 pairs of InGaN/GaN MQWs were grown under a full N_2 atmosphere. The MQWs consist of a 2.5-nm-thick $In_{0.15}Ga_{0.85}N$ well at 720 °C separated by a 12 nm-thick GaN barrier at 820 °C with slight Si doping (electron concentration $= 3 \times 10^{17}$ cm^{-3}). For device A, a 10-nm-thick undoped GaN spacer layer was deposited, followed by a 200-nm-thick Mg-doped GaN layer (hole concentration $\sim 5 \times 10^{17}$ cm^{-3}). For device B, a 200-nm-thick Si-doped GaN layer was used to replace the Mg-doped GaN layer in device A. The electron concentration was identical to that in the 4-μm-thick GaN layer. The MQWs with p–n junction structure were annealed for 20 min at 700 °C under N_2 atmosphere.

Chip fabrication for measurements With standard chip cutting technology, both of the structures were made to a 1 mm×1 mm area size with Ti/Cr/Ni and Ni/Au for the n-type electrode and the p-type electrode, respectively. For light-to-electricity characterizations, a wire bonding system was used with Si/Al wires on the electrodes.

X-ray analysis High-resolution x-ray diffraction (HRXRD-PANalytical X/Pert PRO MPD x-ray diffraction system) was used to analyze the crystalline quality and the thickness of the MQWs.

Light-to-electricity conversion measurements A 405-nm laser diode was used as the excitation source, with a continuously tunable excitation power from 0 to 27 mW. The photoluminescence (PL) measurement system was used in conjunction with a lock-in amplifier to analyze the light-to-electricity process of the two devices. During the experiments for the device structure of MQWs with a p–n junction, the open-circuit voltage and the PL spectrum under open-circuit conditions were measured simultaneously, while the circuit current and the PL spectrum were measured simultaneously under short-circuit conditions. For device B, the circuit current and the PL spectrum were measured simultaneously when

the chip was under a 3 V bias. In the experiment on the dependence of the integrated PL intensity on the circuit current, the circuit series resistance was changed, and the corresponding integrated PL intensity and the circuital current were then measured under 2.4 mW and 27 mW excitation powers, respectively.

References

[1] Green M A 2009 *Prog. Photovoltaics* **17** 183
[2] Dimroth F, Grave M and Beutel P 2014 *Prog. Photovoltaics* **22** 277
[3] Gloeckler M, Sankin I and Zhao Z 2013 *IEEE J. Photovoltaics* **3** 1389
[4] Chirila A, Buecheler S, Pianezzi F, Bloesch P, Gretener C, Uhl A R, Fella C, Kranz L, Perrenoud J, Seyrling S, Verma R, Nishiwaki S, Romanyuk Y E, Bilger G and Tiwari A N 2011 *Nat. Mat.* **10** 857
[5] Rogalski A 2005 *Rep. Prog. Phys.* **68** 2267
[6] Callewaert F, Hoang A M and Razeghi M 2014 *Appl. Phys. Lett.* **104** 053508
[7] Korona K P, Drabińska A, Caban P and Strupiński W 2009 *J. Appl. Phys.* **105** 083712
[8] Chen X, Zhu H, Cai J and Wu Z 2007 *J. Appl. Phys.* **102** 024505
[9] Zhang H, Babichev A V, Jacopin G, Lavenus P, Julien F H, Egorov A Y, Zhang J, Pauporté T and Tchernycheva M 2013 *J. Appl. Phys.* **114** 234505
[10] Grundmann M 2010 *The Physics of Semiconductors* (Heidelberg: Springer-Verlag)
[11] Basu P K 1997 Theory *of Optical Processes in Semiconductors: Bulk and Microstructures* (New York: Oxford University Press)
[12] Barnham K W J, Ballard I, Connolly J P, Ekins-Daukes N J, Kluftinger B G, Nelson J and Rohr C 2002 *Physica E* **14** 27
[13] Gurioli M, Martinez-Pastor J, Colocci M, Deparis C, Chastaingt B and Massies J 1992 *Phys. Rev. B* **46** 6922
[14] Botha J R and Leitch A W R 1994 *Phys. Rev. B* **50** 18147
[15] Levi D H, Wake D R, Klein M V, Kumar S and Morkoç H 1992 *Phys. Rev. B* **45** 4274
[16] Graham D M, Dawson P, Godfrey M J, Kappers M J and Humphreys C J 2006 *Appl. Phys. Lett.* **89** 211901
[17] Fonash S J 2010 *Solar Cell Device Physics* (Burlington: Academic Press/Elsevier)
[18] Miller D A B, Chemla D S, Damen T C, Gossard A C, Wiegmann W, Wood T H and Burrus C A 1984 *Phys. Rev. Lett.* **53** 2173
[19] Nozik A J 2001 *Annu. Rev. Phys. Chem.* **52** 193
[20] Ridley B K 1982 *J. Phys. C: Solid State Phys.* **15** 5899
[21] Smith M, Lin J Y, Jiang H X, Khan A, Chen Q, Salvador A, Botchkarev A, Kim W and Morkoc H 1997 *Appl. Phys. Lett.* **70** 2882
[22] Ng H M, Doppalapudi D, Moustakas T D, Weimann N G and Eastman L F 1998 *Appl. Phys. Lett.* **73** 821
[23] Wang T, Saeki H, Bai J, Shirahama T, Lachab M, Sakai S and Eliseev P 2000 *Appl. Phys. Lett.* **76** 1737
[24] Kaufmann U, Schlotter P, Obloh H, Kohler K and Maier M 2000 *Phys. Rev. B* **62** 10867
[25] Simon J, Protasenko V, Lian C, Xing H and Jena D 2010 *Science* **327** 60
[26] Sze S M 2007 *Physics of Semiconductor Devices* (3rd Edn.) (Hoboken: Wiley-Interscience)
[27] Sun C K, Vallée F, Keller S, Bowers J E and DenBaars S P 1997 *Appl. Phys. Lett.* **70** 2004